Physiological type I collagen organization induces the formation of a novel class of linear invadosomes

Amélie Juin[a,b,c], Clotilde Billottet[a,b,c,*,†], Violaine Moreau[a,b,*], Olivier Destaing[d], Corinne Albiges-Rizo[d], Jean Rosenbaum[a,b,e], Elisabeth Génot[a,b,c,e,*], and Frédéric Saltel[a,b,c,*]

[a]INSERM, U1053 and [b]Université Bordeaux Segalen, F-33076 Bordeaux, France; [c]European Institute of Chemistry and Biology, F-33600 Pessac, France; [d]Institut Albert Bonniot, Université Joseph Fourier, CNRS ERL5284, INSERM, U823, 38042 Grenoble, Cedex 9, France; [e]CHU de Bordeaux, F-33076 Bordeaux, France

ABSTRACT **Invadosomes are F-actin structures capable of degrading the matrix through the activation of matrix metalloproteases. As fibrillar type I collagen promotes pro-matrix metalloproteinase 2 activation by membrane type 1 matrix metalloproteinase, we aimed at investigating the functional relationships between collagen I organization and invadosome induction. We found that fibrillar collagen I induced linear F-actin structures, distributed along the fibrils, on endothelial cells, macrophages, fibroblasts, and tumor cells. These structures share features with conventional invadosomes, as they express cortactin and N-WASP and accumulate the scaffold protein Tks5, which proved essential for their formation. On the basis of their ability to degrade extracellular matrix elements and their original architecture, we named these structures "linear invadosomes." Interestingly, podosomes or invadopodia were replaced by linear invadosomes upon contact of the cells with fibrillar collagen I. However, linear invadosomes clearly differ from classical invadosomes, as they do not contain paxillin, vinculin, and β1/β3 integrins. Using knockout mouse embryonic fibroblasts and RGD peptide, we demonstrate that linear invadosome formation and activity are independent of β1 and β3 integrins. Finally, linear invadosomes also formed in a three-dimensional collagen matrix. This study demonstrates that fibrillar collagen I is the physiological inducer of a novel class of invadosomes.**

Monitoring Editor
Jean E. Schwarzbauer
Princeton University

Received: Jul 5, 2011
Revised: Oct 27, 2011
Accepted: Nov 17, 2011

This article was published online ahead of print in MBoC in Press (http://www.molbiolcell.org/cgi/doi/10.1091/mbc.E11-07-0594) on November 23, 2011.

*C.B. and V.M. contributed equally to this work. E.G. and F.S. contributed equally to this work.

†Present address: INSERM, U1029, F-33400 Talence, France; Université Bordeaux 1, Bordeaux, France.

Address correspondence to: Frédéric Saltel (frederic.saltel@inserm.fr).

Abbreviations used: BAEC, bovine aortic endothelial cell; BHK-21, baby hamster kidney cell line; DDR, discoidin domain receptor; DPBS, Dulbecco's phosphate-buffered saline; ECM, extracellular matrix; FCS, fetal calf serum; FITC, fluorescein isothiocyanate; GFP, green fluorescent protein; GPVI, glycoprotein VI; HFF, human foreskin fibroblast; HPAEC, human pulmonary arterial endothelial cell; HUVEC, human umbilical vein endothelial cell; IRM, interference reflection microscopy; LAIR-1, leukocyte-associated immunoglobulin-like receptor-1; LSEC, liver sinusoidal endothelial cell; MEF, mouse embryonic fibroblast; MMP, matrix metalloproteinase; MT1-MMP, membrane type 1 matrix metalloproteinase; NA, numerical aperture; NaF, sodium fluoride; PAEC, porcine aortic endothelial cell; PDBu, phorbol-12,13 dibotyrate; PMA, phorbol-12 myristate-13-acetate; RT, room temperature; siRNA, small interfering RNA; SVEC4-10, SV40-transformed murine endothelial cell; WT, wild type.

INTRODUCTION

Type I collagen (collagen I) is the most abundant extracellular matrix (ECM) protein in vertebrates. Collagen I molecules are composed of monomeric triple helices, each formed by two α1 and one α2 chains (Epstein and Munderloh, 1975). In the extracellular space, procollagen molecules consist of autoassembled trimers that evolve into fibrils and then into fibers (Elbjeirami *et al*., 2003). Type I collagen monomers are unstable and do not exist in vivo. Fibrillogenesis is necessary to stabilize and confer mechanical properties to fibrils (Shoulders and Raines, 2009; Leitinger, 2011). Collagen I is present in most organs, and abnormalities in collagen I deposition are involved in several diseases, such as tissue fibrosis, osteoporosis, osteogenesis imperfecta, cancer, and atherosclerosis (Prockop and Kivirikko, 1984). On the other hand, collagen remodeling is also required for physiological processes, such as growth, embryogenesis, and wound healing. Degradation of collagen I fibers is mediated by a limited number of enzymes belonging to the matrix metalloproteinase (MMP) family, including MMP-1, MMP-8, MMP-13, and MT1-MMP (Ohuchi *et al*., 1997). At physiological temperature, helical cleavage is followed by spontaneous denaturation of α chains that

are then digested by gelatinase A (MMP-2) and B (MMP-9). In addition, membrane type 1 matrix metalloproteinase (MT1-MMP)–dependent activation of pro-MMP-2 is triggered by collagen I in fibroblasts (Azzam and Thompson, 1992; Theret *et al.*, 1999; Ruangpanit *et al.*, 2002).

Collagen I fibrils as elements of the ECM promote cell adhesion, which is associated with reorganization of the actin cytoskeleton. Actin-based adhesion structures include as major members focal adhesions (Medalia and Geiger, 2010) and invadosomes (Albiges-Rizo *et al.*, 2009). Focal adhesions perform the link between ECM and the actin cytoskeleton. Integrins are major components of focal adhesions and consist of heterodimeric transmembrane receptors composed of α and β subunits that are crucial for cell–matrix interactions. Focal adhesions correspond to a dynamic macro-complex of proteins, including several integrin partners, such as talin, paxillin, and vinculin. Invadosomes are dependent on Src activity and show a dual capacity to interact with and to degrade ECM (Linder, 2007). They are subdivided into two classes of structures: podosomes found in normal cells and invadopodia in transformed and cancer cells (Tarone *et al.*, 1985; Zambonin-Zallone *et al.*, 1988). In cells of the myelomonocytic lineage, such as macrophages, dendritic cells, neutrophils, and osteoclasts, podosomes arise spontaneously upon cell adhesion. Some nonhematopoietic cells can also form podosomes under appropriate stimulation (David-Pfeuty and Singer, 1980; Tarone *et al.*, 1985; VanWinkle *et al.*, 1995; Hai *et al.*, 2002; Moreau *et al.*, 2003; Osiak *et al.*, 2005; Tatin *et al.*, 2006, 2010; Varon *et al.*, 2006; Xiao *et al.*, 2009). Invadopodia were observed constitutively in several invasive cancer cell types, such as metastatic mammary carcinoma cells (Lizarraga *et al.*, 2009), mammary adenocarcinoma (Bravo-Cordero *et al.*, 2011), and melanoma cells (Monsky *et al.*, 1994). Podosomes and invadopodia are highly dynamic actin-based adhesion microdomains formed at the ventral membrane of the cell and able to degrade ECM using MMPs, such as MT1-MMP, MMP-2, and/or MMP-9 (Artym *et al.*, 2006; Guegan *et al.*, 2008). They contain an F-actin core enriched in actin-regulating proteins, including cortactin, N-WASP, and Arp2/3. Invadosomes present a ring (or cloud) around the F-actin core that is composed of actin-associated proteins, such as integrins, vinculin, and paxillin. β1 and β3 integrins have been implicated in invadosome formation and function (Nakahara *et al.*, 1998; Mueller *et al.*, 1999; Pfaff and Jurdic, 2001; Destaing *et al.*, 2010, 2011). Depending on the nature of the associated α chain, β1 and β3 integrins behave as collagen or laminin receptors and vitronectin receptor, respectively. Invadopodia of cancer cells and podosomes of normal cells exhibit some distinct features. Invadopodia consist of a low number of small F-actin dots (1–10 with diameters of 1–2 μm) with a long lifetime (more than 1 h) and a high protrusive capacity. On the other hand, podosomes can be found in individual dots or self-organized in large structures, aggregates (20–200 podosomes), or rosettes (with 10–100 μm diameter) with a short lifetime (around 2–12 min; Destaing *et al.*, 2003; Linder, 2007). Podosomes and invadopodia can be formed on different ECM substrates, such as vitronectin, fibronectin, collagen type IV, and laminin (Kelly *et al.*, 1994; Linder, 2007; Destaing *et al.*, 2011). Although experiments have revealed that adhesion via ECM components is necessary for invadosome formation and modulation (Sabri *et al.*, 2006; Destaing *et al.*, 2010; Liu *et al.*, 2010; Nascimento *et al.*, 2011), none describe the physiological organization of one matrix component as an invadosome inducer. Because collagen I fibrils are among the major microenvironmental components to which cells are exposed in vivo, and due to their capacity to activate MT1-MMP, and consequently pro-MMP-2, the goal of this study was to analyze the impact of fibrillar collagen I on invadosome formation.

RESULTS

Fibrillar collagen I induces linear F-actin structures

Since primary liver sinusoidal endothelial cells (LSECs) in fibrotic liver are exposed to an unusual abundance of ECM components, including collagen, we started this study with LSECs. To test how collagen I accumulation affects the actin cytoskeleton, primary LSECs were seeded on glass coverslips coated with collagen I fibrils or different ECM components. After 24 h, confocal analysis of LSEC cytoskeleton revealed the presence of linear F-actin structures in cells grown on collagen I coating (0.2 mg/ml coated at room temperature [RT]; Figure 1A). These structures were collagen I–specific; none of the other individual ECM components tested, such as collagen IV, collagen III, and laminin, led to the same F-actin organization (Figure 1B; unpublished data). Approximately 50% of LSECs exhibited these structures. Collagen I induced their formation in a dose-dependent manner (Supplemental Figure S1A). The number and the length of these structures varied from 1 to 10 per cell and from 0.5–5 μm, respectively. A Z-stack analysis showed that they localized at the basal part of the cells (Figure S1B).

Collagen I exists in different forms: gelatin (denatured collagen I), monomeric (in acidic condition), and fibrils, as in vivo. Temperature, pH, and time control collagen I fibrillogenesis and, consequently, the type of coating obtained (Wood and Keech, 1960; Cooper, 1970). To explore whether the formation of these structures is dependent on a specific collagen I organization, three distinct coating conditions were tested, each corresponding to a stepwise increase in collagen I fibrillogenesis at a constant collagen I concentration (0.2 mg/ml). Collagen I fibrillogenesis was verified by interference reflection microscopy (IRM; Figure 1C). These experiments showed that linear F-actin structures were induced only in the presence of collagen I fibrils corresponding to the physiological form of collagen I. When fibrillogenesis was performed at RT, 50% of cells exhibited these structures, and the cell count increased to 80% at 37°C (Figure 1D). By using collagen I-fluorescein isothiocyanate (FITC), we confirmed with confocal microscopy, which incorporated Z-stack observation and three-dimensional reconstruction, that formation of these structures occurred only along collagen I fibrils (Figure 1E). Our results demonstrate that collagen I fibrils induced specific F-actin reorganization into linear structures in LSECs.

Next we addressed the question of cell specificity in the formation of linear F-actin structures in a collagen I fibril context. Several endothelial cell types from different species and vascular beds were seeded on collagen I fibrils to examine their ability to form these structures. Human umbilical vein endothelial cells (HUVECs), bovine aortic endothelial cells (BAECs), human pulmonary arterial endothelial cells (HPAECs), SV40-transformed murine endothelial cells (SVEC4-10), and M1 cells (a murine LSEC cell line) exhibited the same linear F-actin organization (Figure S2, A and B; unpublished data). Only porcine aortic endothelial cells (PAECs) proved unable to form these structures in contact with collagen I fibrils (Figure S2C). So, independent of the vascular beds and species, most endothelial cells are able to form these linear F-actin structures. We found that other cell types, such as primary human foreskin fibroblasts (HFFs), the fibroblast baby hamster kidney cell line (BHK-21), and mouse embryonic fibroblasts (MEFs) also presented linear F-actin structures in a collagen I context (Figure S2, D–F). We noticed differences in the percentage of cells exhibiting these linear F-actin structures depending on the cell type (Figure S2). This nonexhaustive analysis showed that fibroblasts and endothelial cells are able to reorganize their actin cytoskeleton into linear F-actin structures upon contact with collagen I fibrils.

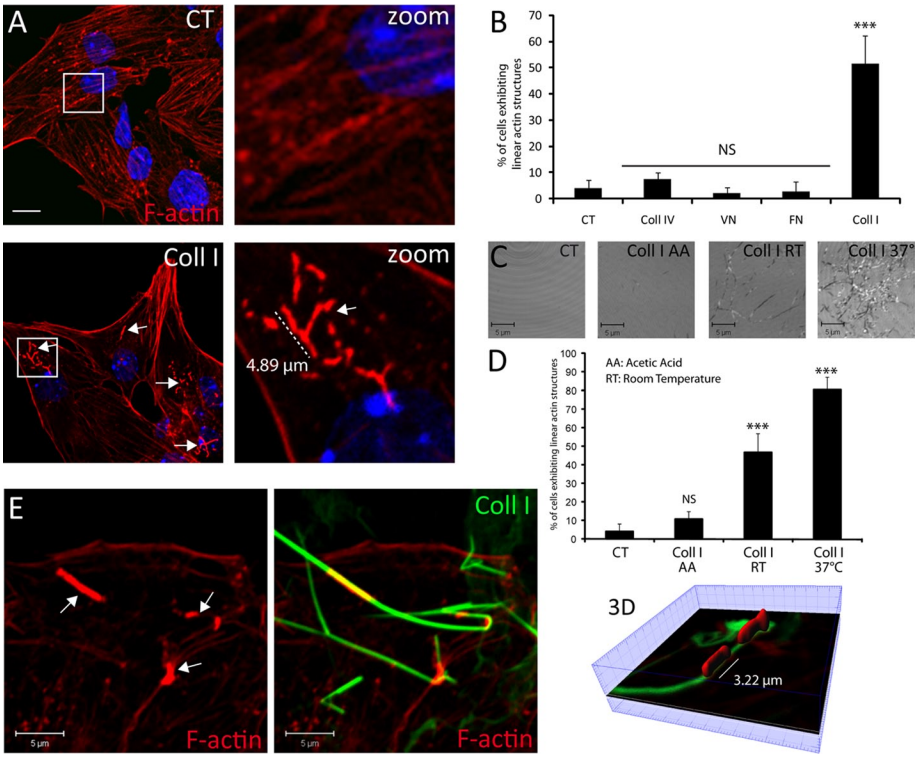

FIGURE 1: Fibrillar collagen I induces linear F-actin structures. (A) Representative confocal microscopy images of linear F-actin structures (white arrows) associated with a reorganization of actin cytoskeleton in LSECs on collagen I matrix. Control cells (CT) were seeded on glass. F-actin (red) and nuclei (blue) were stained respectively with phalloidin and Hoechst. Right panels show zoom of the white squares. Scale bar: 7 µm. (B) Linear F-actin structures are observed only on collagen I. Shown is the percentage of LSECs presenting linear F-actin structures. Results are expressed as mean ± SD. (n = 200; three experiments; ***$p < 0.001$). (C) IRM images showing control (CT = glass) and acetic acid (AA) at room temperature (Collagen I RT) or 37°C (Collagen I 37°C) conditions of collagen I coating. Neutral pH and warmer conditions increased fibrillogenesis. Scale bar: 5 µm. (D) Collagen I fibrillogenesis induces the formation of linear F-actin microdomains. Shown is the percentage of LSECs presenting linear F-actin structures (mean ± SD; n = 200; three experiments; *** $p < 0.001$ as compared with control). (E) Confocal images of LSECs on fibrillar collagen-FITC (green). Actin structures (white arrows) are formed exclusively along collagen I fibrils. Scale bars: 5 µm. A three-dimensional reconstruction shows the association between linear F-actin structures (red) and collagen I fibers (green).

Affiliation of collagen I–induced linear F-actin structures with invadosomes

To test whether these linear F-actin structures could correspond to invadosomes, we first analyzed their molecular composition. BAECs (Figures 2A and S3A) and LSECs (Figure S3B) were seeded on collagen I fibrils and immunolabeled with antibodies against classical markers of invadosomes. First, these linear F-actin structures stained positively for phosphotyrosine all along the structures delineated by F-actin staining (Figures 2A and S3B). They were also positive for N-WASP, the actin nucleator Arp2/3, and cortactin (Figures 2A and S3, A and B). Interestingly, some markers of invadosomes shared with focal adhesions, such as paxillin and vinculin, were not observed in these structures (Figures 2A and S3A). The scaffold protein Tks5, known to be an Src substrate and implicated in invadopodia formation but not in focal adhesions (Abram *et al.*, 2003), was also concentrated in these structures (Figures 2A and S3B). Tks5 was used as marker of these structures in the rest of the study.

We then explored the impact collagen I fibrils have on cells exhibiting constitutive invadosomes. To address this point, we used Src-3T3 cells, which express constitutively activated Src and spontaneously exhibit rosettes on glass (Figure 2B). When seeded on collagen I fibrils, they showed linear F-actin structures (Figure 2B). In these conditions, a similar linear rearrangement could be noticed with invadopodia of the MDA-MB-231 breast tumor cell line and with the podosome rosettes of the RAW 264.7 monocyte cell line (Figure 2, C and D). These results underscore the link between these F-actin structures and invadosomes.

Tks5 is required for collagen I–induced linear F-actin structure formation

Tks5 is the most efficient marker for detecting these collagen I–induced linear F-actin structures. When the various cell types examined for their formation were tested for Tks5 expression by Western blotting, no signal could be detected in PAECs, the only endothelial cells unable to form these structures (Figure 3A). This finding prompted us to test whether Tks5 could be involved in PAEC formation. PAECs were transfected with a full-length Tks5-green fluorescent protein (GFP) construct or GFP alone as control (Figure 3B) and seeded on collagen I fibrils. Using GFP as a transfection reporter, we could observe formation of collagen I–induced linear F-actin structures only in PAECs transfected with Tks5 (Figure 3C) compared with PAECs transfected only with GFP (Figure 3D). So, the expression of Tks5 in PAECs proved sufficient to induce linear F-actin structure formation upon contact with collagen I fibrils.

We then used two specific small interfering RNAs (siRNAs) to silence Tks5 in BAECs. Tks5-depleted BAECs (Figure 3E) were seeded on collagen I fibrils to assess their capacity to form linear F-actin structures. The proportion of cells exhibiting these structures was reduced with both Tks5 siRNAs, with a correlation between siRNA efficiency and the impairment. In addition, the number and size of the remaining linear F-actin structures decreased dramatically (unpublished data). These data suggest that a low level of Tks5 is sufficient to induce linear F-actin structure formation. Moreover, Tks5 overexpression in BAECs and PAECs, was not sufficient to promote their induction in the absence of collagen I fibrils, showing the absolute requirement of both Tks5 and collagen I fibrils for their formation. Altogether, these results underline the central role of Tks5 in the formation of these collagen I–induced linear F-actin structures, a situation similar to that reported for invadopodia formation in Src-transformed cells (Seals *et al.*, 2005).

Fibrillar collagen I induces linear functional invadosomes

Matrix-degrading capacity is the hallmark of invadosomes. To test whether these collagen I–induced linear F-actin structures were able to degrade ECM, BAECs were seeded on a mixed gelatin/collagen I fibril matrix. This led to the formation of linear F-actin structures along collagen I fibrils and associated gelatin degradation, which was not the case on gelatin alone (Figure 4, A–D). On this mixed matrix, which combined gelatin-FITC to monitor degradation and collagen I fibrils

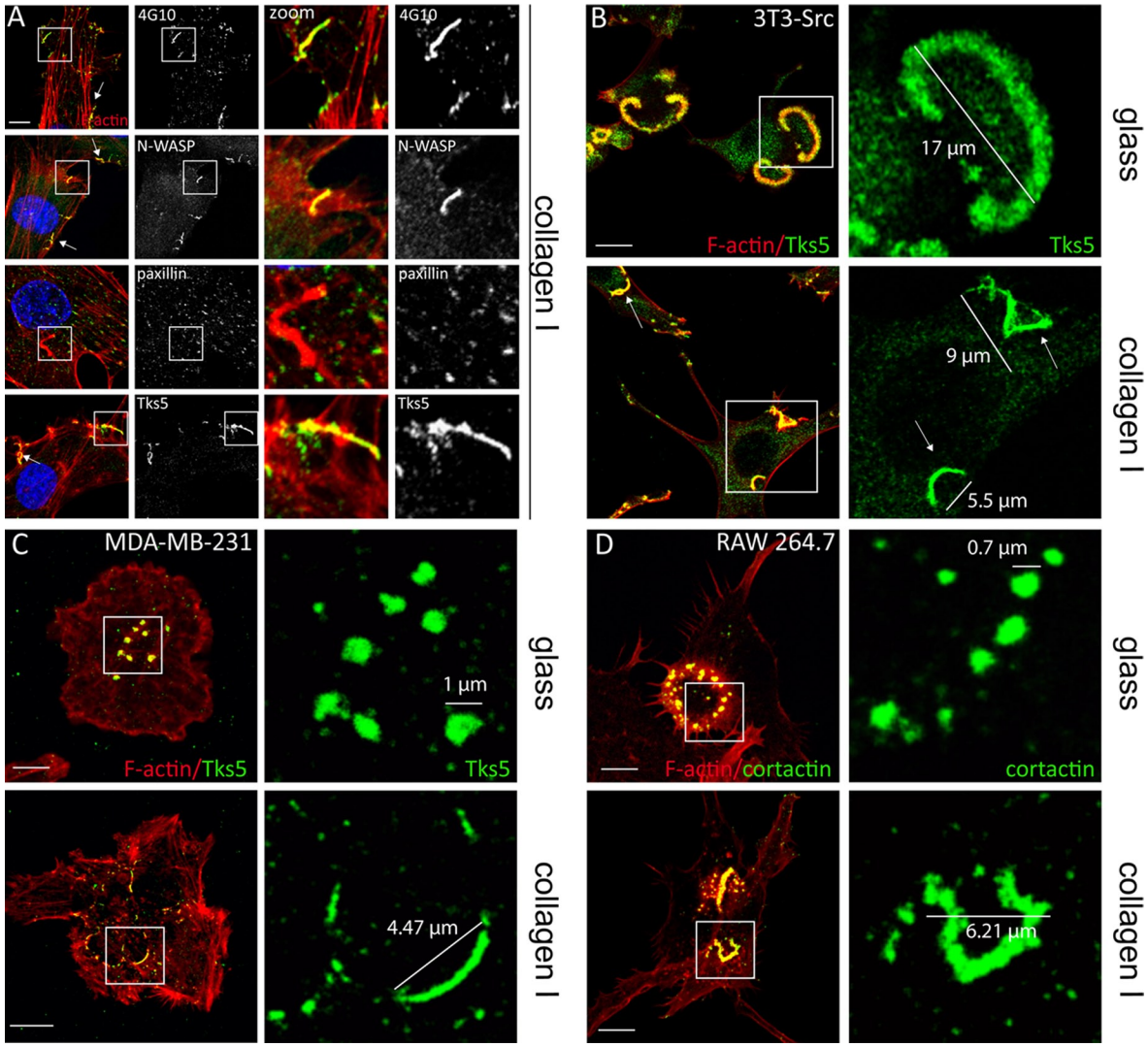

FIGURE 2: Molecular characterization of linear F-actin structures induced in the presence of collagen I fibrils. (A) BAECs were seeded on 0.4 mg/ml fibrillar collagen I and processed for fluorescent staining: F-actin (red), nuclei (blue), and invadosome markers (green), such as phosphotyrosine (4G10), N-WASP, paxillin, and Tks5. Merged image indicates colocalization of linear F-actin structures with phosphotyrosine, N-WASP, and Tks5, but not with paxillin. In zoom of white square (3.5×) colocalization of phosphotyrosine and paxillin can be noted with focal adhesions at the extremity of stress fibers. N-WASP and Tks5 colocalize with linear F-actin structures but not with focal adhesions. Scale bar: 5 µm. (B) Top panel, Src-3T3 cells seeded on glass coverslips exhibited classical "rosettes." F-actin: red; Tks5: green. Scale bar: 10 µm. Right, zoom (3.5×) of the white square shows the presence of Tks5 in a "rosette." Bottom panel, Src-3T3 cells were seeded on collagen I fibrils and exhibited linear F-actin structures (white arrows) F-actin: red; Tks5: green. Scale bar: 10 µm. Right, zoom (3×) of the white square shows a localization of Tks5 in collagen I–induced structures (white arrows). (C) MDA-MB-231 were seeded on glass coverslips, where invadopodia were observed (top panel), and on collagen I fibrils, where invadopodia were linearized (bottom panel). F-actin: red; Tks5: green. Scale bars: 10 µm. Zoom: 4.4×. (D) RAW 264.7-derived macrophages form rosettes of podosomes on glass coverslips (top panel, scale bar: 5 µm) and F-actin structures on collagen I fibrils (bottom panel, scale bar: 6 µm). F-actin: red; cortactin: green. Zoom; 4.4×.

to induce formation of these structures, more than 70% of the cells exhibited linear F-actin structures along fibrils and 86 ± 9% of cells were associated with a degradation activity (unpublished data). The same gelatin degradation activity was also observed in LSEC and in PAECs transfected with Tks5-GFP (Figure S4, A and B).

Linear F-actin structures formed on mixed matrix stained strongly for MT1-MMP, the major activator of pro-MMP-2 (Figure 4E). By using zymography on cell lysates, we confirmed that growing BAECs on collagen I fibrils led to the activation of pro-MMP-2 (Figure S4C). Seeding cells on fibrillar collagen I did not alter MT1-MMP expression (Figure S4D). However, the degradative activity was not necessary for the formation of these structures, since cells treated with the MMP inhibitor GM6001 still form linear F-actin structures (Figure 4F). Likewise, the number and fractional cell surface area of these F-actin structures were not significantly different between wild-type (WT) and MT1-MMP$^{-/-}$ MEFs, although they lacked a degradation activity (Figure S4, E and F). Thus, MT1-MMP, although not required for the formation of these structures, is necessary for their degradation activity.

Owing to the capacity of MT1-MMP to degrade collagen I fibrils, we investigated the impact these structures have on fibrils themselves. Collagen I labeled with succinimidyl-ester-568 was used to

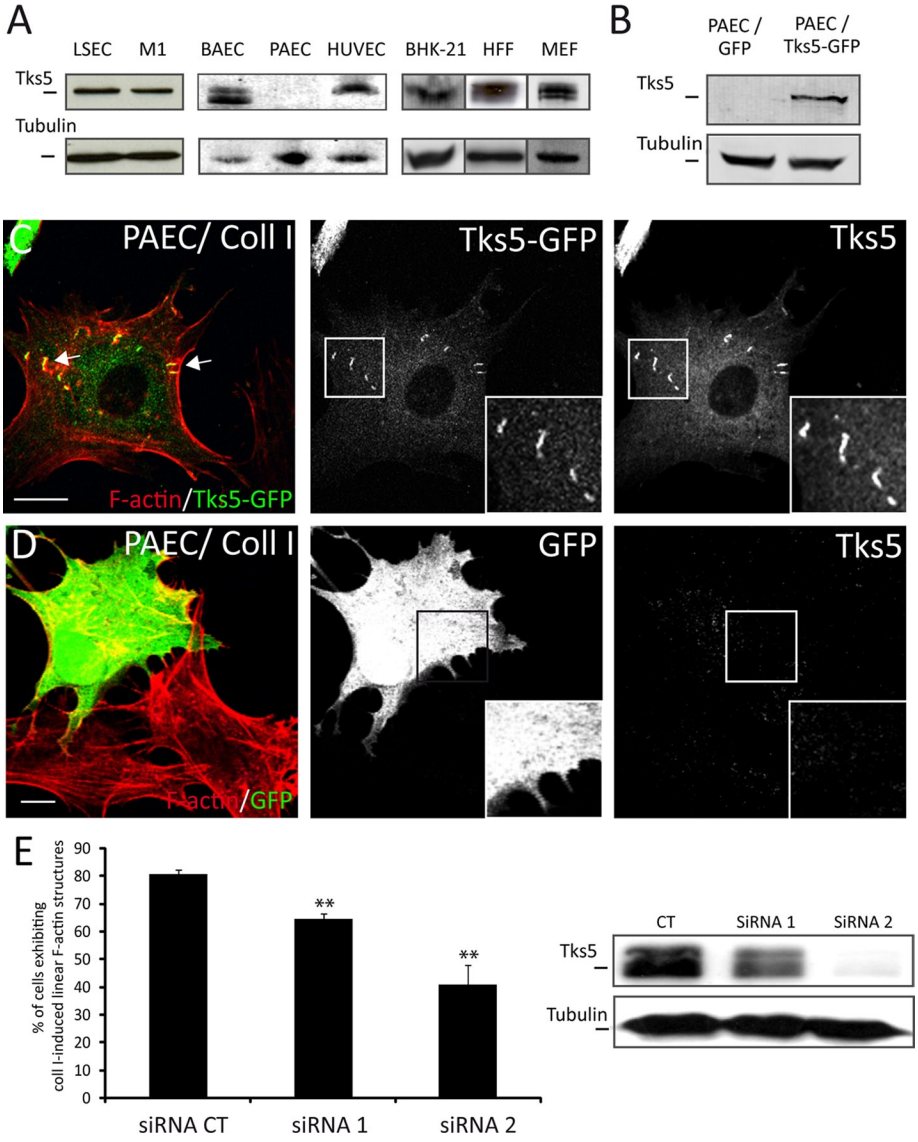

FIGURE 3: Tks5 is required for collagen I–induced linear F-actin structure formation. (A) Protein extracts were analyzed by Western blotting. All cell types tested express Tks5, with the exception of PAECs. Tubulin content is shown as a loading control. (B) Immunoblot showing Tks5 expression level in PAECs transiently transfected with Tks5-GFP or GFP alone. (C) PAECs transiently transfected with a Tks5-GFP present linear F-actin structures on collagen I fibril matrix. F-actin (red) colocalizes with Tks5-GFP construct in these structures (white arrows). Insets are zoomed images of white squares. Scale bar: 10 µm. (D) PAECs were transfected with a GFP control construct unable to promote formation of these structures. Insets are zoomed images of white squares. Scale bar: 10 µm. (E) BAECs were transfected with a control siRNA (CT) or an siRNA targeting Tks5 (siRNA1 or siRNA2). Cells with a down-regulated expression of Tks5 present a decrease in linear F-actin structure formation. Shown is the percentage of BAECs presenting collagen I–induced actin structures ± SD (n = 1200; three experiments; ** $p < 0.01$). Protein extracts of BAECs transfected with indicated siRNA were analyzed by Western blotting.

follow the evolution of fibrils during cell culture. At 24 h after seeding, no degradation of collagen I fibrils was observed (Figure 4G). After 3 d, we observed a decrease of collagen I fibril density, and degradation was complete after 6 d. These data suggest that these linear F-actin structures are able to degrade collagen I fibrils.

We then examined whether the linear reorganization of invadosomes was induced in Src-3T3 cells when they were placed on collagen I fibrils. This condition was compatible with a degradation capacity. We found that Src-3T3 cells, after seeding on mixed matrix, show linear structures associated with gelatin degradation (Figure 5A) and with activation of pro-MMP-2 (Figure S4G). Moreover, collagen I fibrils strongly increased the cell proteolytic activity compared with gelatin alone (Figure 5B). Although, as noted earlier (Figure 3B), linear structures were predominantly observed on collagen I fibril conditions 4 h after seeding (Figure 5, C and D), the situation was reversed 24 h after seeding, with the presence of a majority of invadosome "rosettes" (Figure 5, C–E). This suggests that collagen I fibrils have been degraded by 24 h, thus allowing invadosome rosettes to reform. This was supported by experiments using succinimidyl-ester-568–labeled collagen I (Figure 5, D and E).

Altogether, our results show that these structures correspond to a new linear organization of invadosomes. Owing to their specific and original architecture we named them "linear invadosomes."

Linear invadosome kinetics and dynamics

To further characterize linear invadosomes, we explored their induction delay after cells were seeded on collagen I fibrils. BAECs were transfected with a Ruby Lifeact construct to observe linear invadosome formation during the cell adhesion process. Supplemental Movie S1 shows that linear invadosomes were already evident at the first step of adhesion. F-actin/Tks5 costaining on fixed cells confirmed this finding, indicating the presence of linear invadosomes only 15 min after seeding (Figure 6A). These data suggest an involvement of linear invadosomes in early steps of cell adhesion and/or spreading in collagen I fibril conditions.

To analyze linear invadosome dynamics, BAECs were transfected with Tks5-GFP (Figure 6, B and C). This demonstrated a lifespan of more than 1 h, comparable with that of invadopodia, but much longer than that of podosomes (~2–4 min lifespan; Movie S2). To improve this dynamics analysis and to make sure that we indeed were observing linear invadosomes, we simultaneously visualized collagen I fibrils and linear invadosomes labeled with succinimidyl-ester-568 and Tks5-GFP, respectively. This analysis revealed two distinct situations for linear invadosomes: some appeared static (Figure 6B), whereas others were motile (Figure 6C). Interestingly, linear invadosome movements were highly correlated with those of collagen I fibrils. When the fibril was immobile, the linear invadosome was static. Conversely, when the fibril moved, linear invadosomes followed the fibril shift (Figure 6C and Movies S3, S4, and S5), suggesting a tight interaction between collagen I fibrils and linear invadosomes.

Linear invadosomes are independent of β1 and β3 integrins

β1 and β3 integrins, and associated adhesive proteins, such as vinculin and paxillin, characterize classical invadosomes (Nakahara

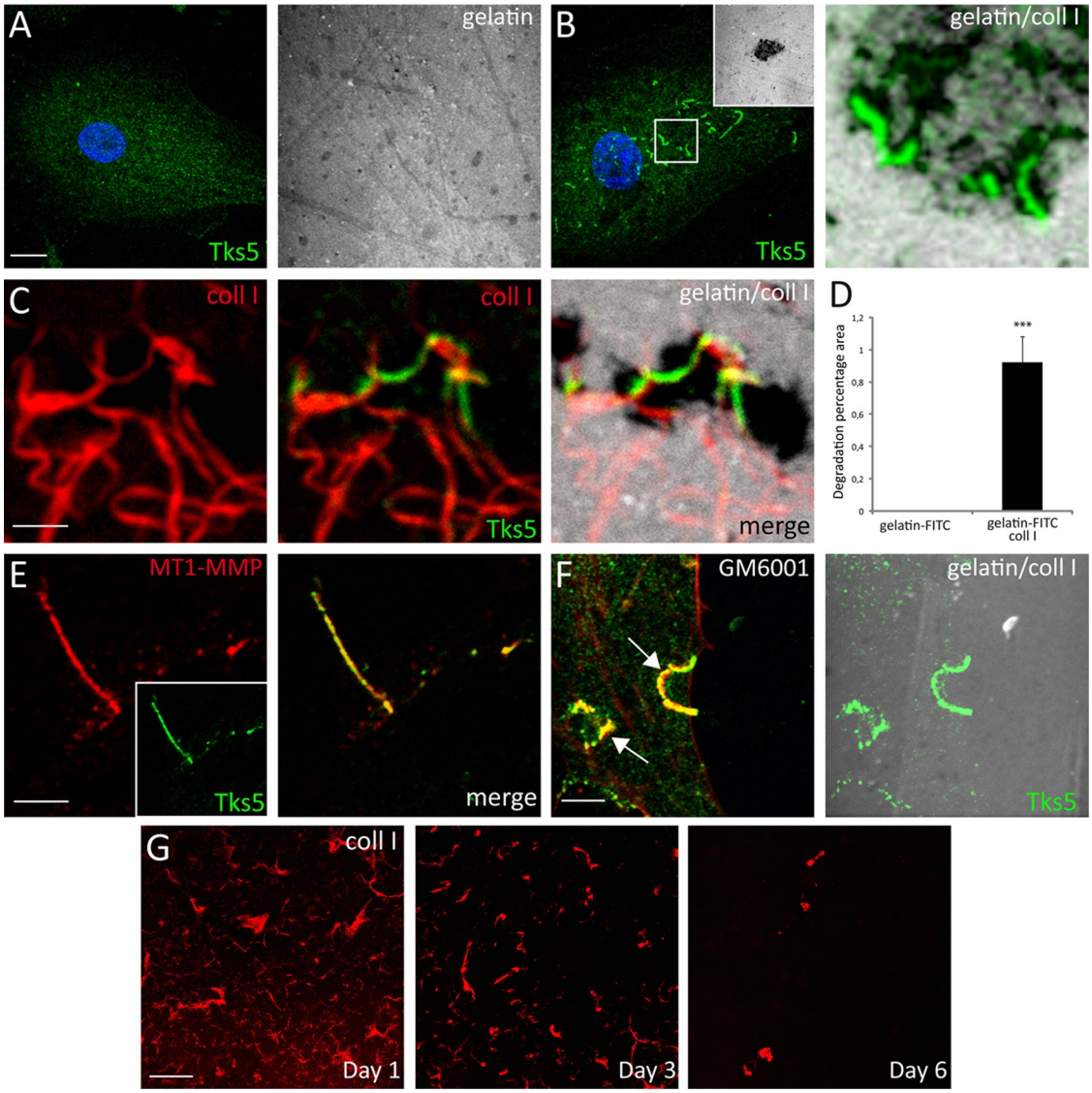

FIGURE 4: Degradation activity of collagen I–induced linear F-actin structures in BAECs. (A and B) BAECs were seeded on fluorescent gelatin-FITC or on a mixed matrix (gelatin-FITC + collagen I fibrils) and stained for Tks5 (green) and nuclei (blue). After 24 h, BAECs show degradation activity of gelatin only on the mixed matrix containing collagen I fibrils. Scale bar: 10 μm. (C) To confirm the association of linear F-actin structures with the degradation activity, BAECs were seeded on a mixed gelatin/collagen matrix with collagen I fibrils labeled with succinimidyl-ester-568. Linear F-actin structures were formed along fibrils and a degradation area were observed underneath. Scale bar: 5 μm. (D) Quantification of the degradation activity that was observed only in the collagen I fibril condition (mean ± SD; n = 100; three experiments; *** $p < 0.001$ compared with control gelatin/collagen I fibrils). (E) Tks5 (green) and MT1-MMP (red) colocalize in the linear F-actin structures formed in BAECs on the mixed matrix. Scale bar: 5 μm. (F) In the same condition (gelatin/collagen I fibrils), BAECs were treated overnight with the MMP inhibitor GM6001 at 5 μM. Scale bar: 5 μm. (G) For analysis of collagen I fibril degradation, BAECs were seeded on collagen I fibrils labeled with succinimidyl-ester-568. No degradation of collagen I fibrils can be observed after 24 h. After 3 d, the density of collagen I fibrils decreased, and after 6 d, the degradation was complete. Scale bar: 35 μm.

et al., 1998; Pfaff and Jurdic, 2001; Badowski *et al.*, 2008; Destaing *et al.*, 2010). During the molecular characterization of linear invadosomes we found that they lacked paxillin and vinculin (Figures 2A and S3A). This result prompted us to investigate the presence and the exact role of integrins in linear invadosome formation and function. First, we found that although β1 and β3 integrins were easily detected by immunostaining at focal adhesions, they did not colocalize with linear invadosomes (Figure 7, A and B). In the majority of cases, there was no connection between focal adhesion and linear invadosomes. These data, consistent with the absence of vinculin and paxillin, demonstrate a major difference between linear invadosomes and classical invadosomes.

Because β1 integrin is important for invadosome formation and corresponds to the major receptor implicated in collagen recognition, and despite its lack of localization to linear invadosomes, we used several approaches to test whether it might be somehow involved in linear invadosome formation. cRGD peptide, a blocking integrin peptide, and its control cRAD were added to MEFs (Cardarelli *et al.*, 1994). This did not impede linear invadosome formation, even though cRGD peptide inhibited cell spreading

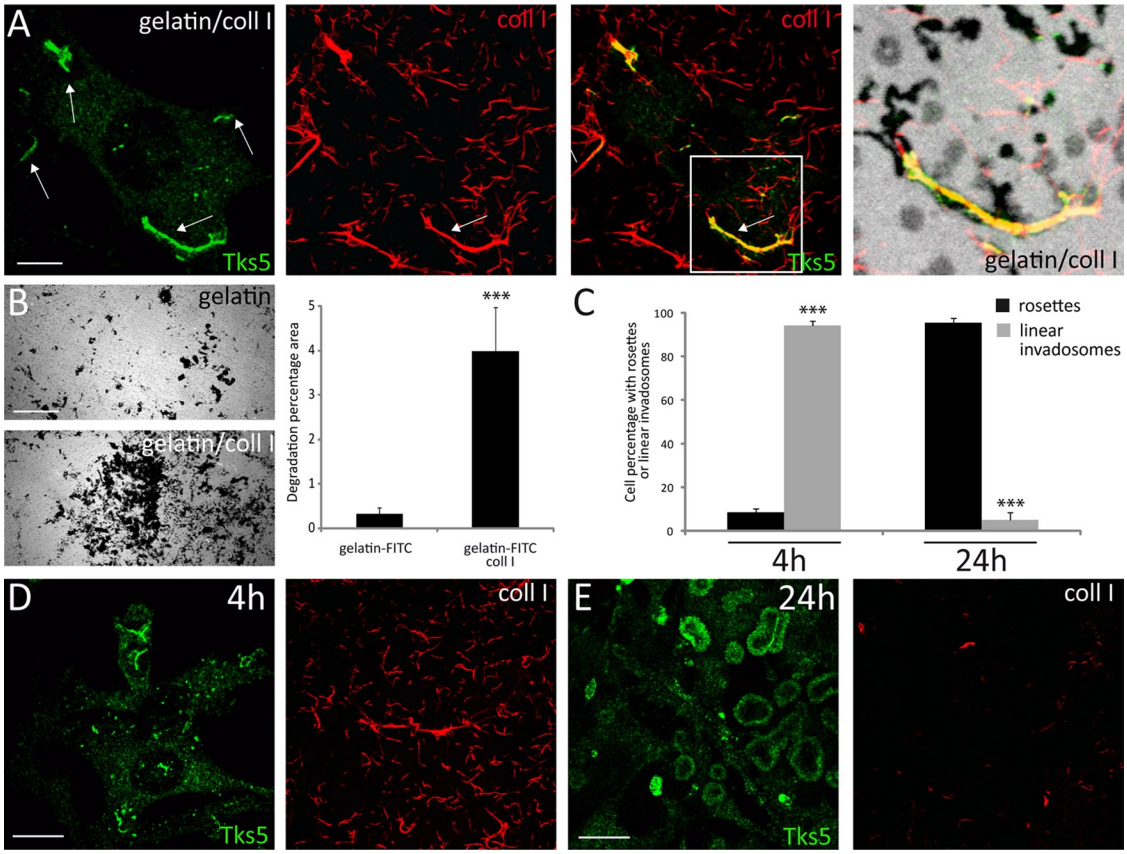

FIGURE 5: Degradation activity of collagen I–induced linear F-actin structures in Src-3T3 cells. (A) Src-3T3 cells were seeded on a mixed matrix of fluorescent gelatin/fluorescent collagen I. Linear structures (white arrows) in Src-3T3 cells are associated with fibrils and degradation area of gelatin. Collagen I: red; Tks5: green; gelatin-FITC: gray. (B) Four hours after seeding, cells were fixed and analyzed for gelatin degradation (in situ zymography). Src-3T3cells are able to degrade gelatin. Gelatin-FITC: gray; degradation area: black. However, on the mixed matrix, the presence of collagen I fibrils is seen to enhance the degradation activity compared with gelatin alone (mean ± SD; n = 30; three experiments; *** $p < 0.001$ compared with control). Scale bar: 20 μm. (C) Quantification of cells exhibiting linear structures and rosettes on mixed matrix after 4 and 24 h (n = 300; three experiments; *** $p < 0.001$ compared with control). (D and E) Src-3T3 cells were seeded on fluorescent collagen I. Four hours after seeding, the majority of cells exhibits linear structures, and collagen I fibrils are maintained (D). Twenty-four hours after seeding, most collagen I fibrils have been degraded. This is concomitant with reformation of classical rosettes in most cells (E).

(Figure S5, A and B). The same result was obtained using the blocking antibody anti-β1 (unpublished data). We then used $\beta3^{-/-}$ and $\beta1^{-/-}$ MEFs that were compared with WT MEFs. The expected integrin expression in knockout MEFs was verified by immunostaining (Figure S5, C and D). As did other cell types, WT MEFs readily formed linear invadosomes with a matrix-degrading activity only when seeded on collagen I fibrils (Figure 7, C and D). Identical results were obtained with $\beta1^{-/-}$ and $\beta3^{-/-}$ MEFs, demonstrating that neither β1 nor β3 are necessary for the formation and activity of linear invadosomes (Figure 7, E and F). The total number of linear invadosomes per square micrometer and the fraction of the cell surface occupied by these structures were found to be similar in WT, $\beta3^{-/-}$, and $\beta1^{-/-}$ MEFs (Figure 7, G and H and Supplemental Table S1). On the mixed gelatin/collagen I matrix, 100% of WT and knockout MEFs were associated with degradation areas.

These data show that neither β1 nor β3 integrins are necessary for linear invadosome formation and activity. Consequently, linear invadosomes represent a new class of invadosomes, with an original linear morphology, β1 and β3 integrin independence, and a unique sensitivity to collagen I architecture.

Linear invadosome formation in a three-dimensional environment

In vivo, cells evolve in a three-dimensional environment, with ECM contacts on every side of the cell. Recent studies observed formation and organization of podosomes in three dimensions (Li *et al.*, ; Van Goethem *et al.*, 2010). To test the presence of linear invadosomes in three dimensions, we seeded BAECs on top of a thick collagen I coating, which they invaded; collagen I fibrils were found both at the apical and basal part of cells (Figure 8, A–C). In this condition, linear invadosomes could be observed independently of the cell polarity (Figure 8, B and C), contrary to focal adhesions stained for integrin β1 that were observed only at the ventral surface of the cell. To confirm the presence of linear invadosomes in three-dimensional conditions, cells were included in a fibrillar collagen I matrix for 24 h. Labeling for F-actin and Tks5 showed that they were still able to form linear invadosomes (Figure 8D). These observations clearly show that linear invadosomes can form in a three-dimensional setting with the only requirement being the contact with collagen I fibrils.

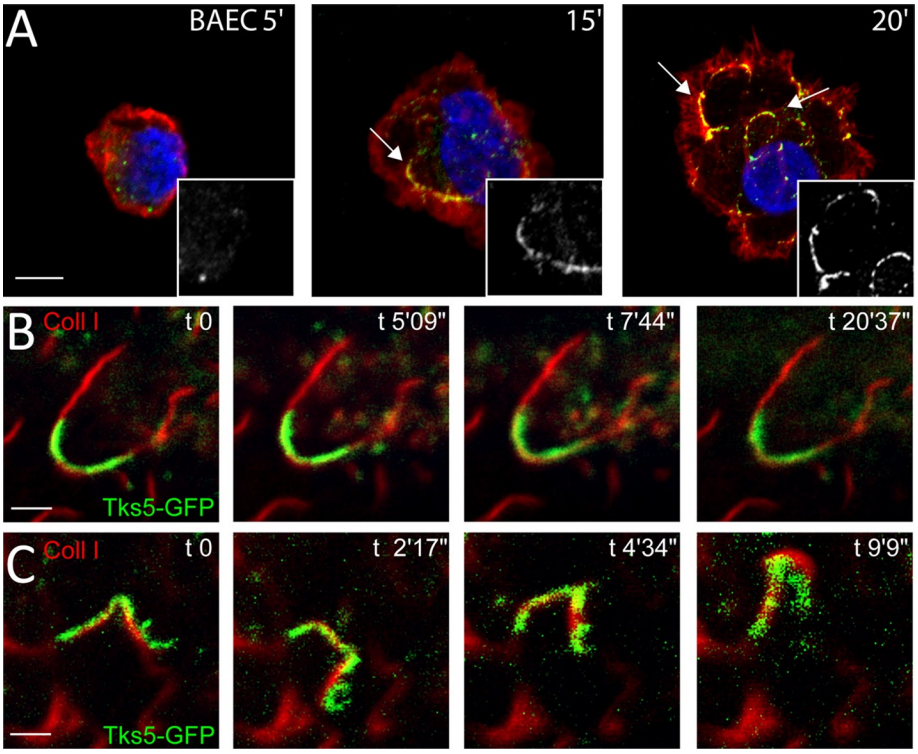

FIGURE 6: Linear invadosome kinetics and dynamics. (A) Linear invadosomes (white arrow) appear in the early stage of adhesion (from 15 min) on fibrillar collagen I. F-actin: red; Tks5: green; nuclei: blue. Scale bar: 7 μm. (B and C) Images from time-lapse video microscopy of BAECs transfected with Tks5-GFP (green) on fibrillar collagen I (red) showing static (B) and motile (C) linear invadosomes. Scale bar: 2 μm.

DISCUSSION

This study has revealed the existence of a new organization of invadosomes, with a specific linear architecture, selectively and specifically induced by the physiological fibrillar organization of collagen I, in a β1- and β3-independent manner. These structures, which we named "linear invadosomes," were observed for the first time in primary LSECs in which the original organization of the actin cytoskeleton, and more precisely the low abundance of stress fibers, helped us to detect them. We were then able to find them in other cell types, even in the presence of a high level of stress fibers, thanks to their accumulation of the scaffold protein Tks5, which has been proven essential for their formation. Indeed, linear invadosomes were observed in all cell types examined, including, as described here, endothelial cells from various vascular beds, macrophages, fibroblasts, and tumor cells. However, the percentage of cell-forming linear invadosomes and the level of associated degradation vary from cell type to cell type. As linear invadosomes may result from the association of multiple protein partners and integration of different molecular events, we assume that this difference reflects the variation of their contributions according to cell type.

Linear invadosomes are inducible structures strictly dependent on the presence of collagen I fibrils. They were assembled within minutes upon contact with collagen I fibers. This is notably faster than the induction delay of invadosomes by soluble agents, which is variable, being 6 h with transforming growth factor β for BAECs (Varon *et al.*, 2006) or 30 min to 1 h with phorbol-12 myristate-13-acetate (PMA), phorbol-12,13 dibotyrate (PDBu), and sodium fluoride (NaF) for different cell types, such as endothelial and smooth muscle cells (Hai *et al.*, 2002; Tatin *et al.*, 2010). In addition, following induction, the number of podosomes starts to decrease after 30 min to 1 h upon PMA or PDBu treatment (Hai *et al.*, 2002; Tatin *et al.*, 2010), whereas linear invadosomes appear stable for up to several hours. Altogether, this suggests that the contact with collagen I fibers is sufficient to assemble and stably maintain the invadosome machinery, F-actin and associated proteins, such as Tks5 and metalloproteinases.

Dynamic observations clearly demonstrated movements of fibrils associated with those of linear invadosomes, suggesting a strong link between both structures. However, whereas every linear invadosome is associated with a type I collagen fibril, it is important to notice that every collagen I fibril does not induce linear invadosome formation. This observation suggests that the nature, density, diameter, and, potentially, the cross-linking level of the fibril may be involved in linear invadosome formation. Whereas it has already been shown that collagen matrix architecture dictates three-dimensional migration modes of human macrophages (Van Goethem *et al.*, 2010), we show that collagen I architecture also induces the linear invadosome formation.

As integrins are the major receptors for collagen and are found associated to podosomes and invadopodia, we took great care to examine the presence and function of integrins in linear invadosomes. Using immunocytochemistry, integrin-deficient cells, and RGD peptide, we show that β1 and β3 integrins are not localized within linear invadosomes, nor are they necessary for linear invadosome formation and activity. The lack of β1 and β3 integrins in linear invadosomes thus reflects a major difference between linear invadosomes and other invadosomes and raises the question of the identity of the collagen receptor responsible for linear invadosome formation.

At this time, four major classes of vertebrate transmembrane receptors are known to interact directly with the native collagen triple helix: collagen-binding β1 integrins, discoidin domain receptors (DDRs), glycoprotein VI (GPVI), and leukocyte-associated immunoglobulin-like receptor-1 (LAIR-1; Leitinger and Hohenester, 2007). Our data eliminated β1 and β3 integrins. Since GPVI is present only on platelets and LAIR-1 on leukocytes, we turned our attention to DDRs, which are ubiquitously expressed. Our preliminary data seem to exclude a role for DDRs since: 1) LSECs isolated from DDR2$^{-/-}$ mice (Labrador *et al.*, 2001) were still able to form linear invadosomes to the same extent as WT LSECs (unpublished data); and 2) nilotinib and imatinib, which potently inhibit the kinase activity of both DDR1 and DDR2 receptors (Day *et al.*, 2008), did not affect the formation of linear invadosomes in cells exposed to type I collagen fibrils (unpublished data). We also ruled out the role of CD44, another type of collagen I receptor (Jalkanen and Jalkanen, 1992) known to play an important role in podosome formation in osteoclasts (Chabadel *et al.*, 2007), since CD44$^{-/-}$ MEFs (Shi *et al.*, 2006) did not show any defect in linear invadosome formation (unpublished data). Further work is required to identify the collagen I receptor involved in the formation of linear invadosomes. In addition, redundancy and association between receptors, including with other classes of integrins, need to be considered to fully

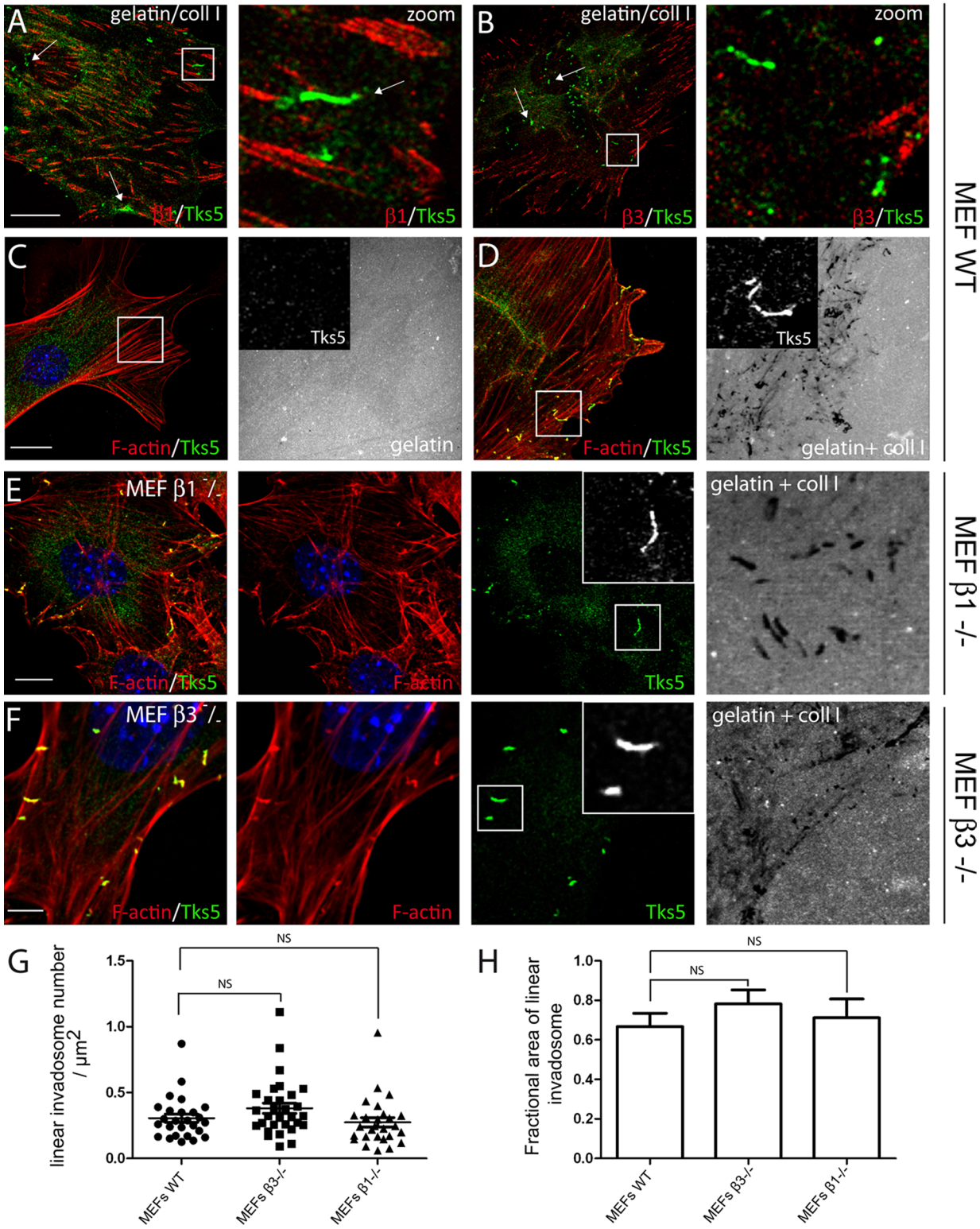

FIGURE 7: Linear invadosomes, a new class of β1 and β3 integrin–independent invadosomes. (A and B) MEFs were seeded on a mixed gelatin-FITC/collagen I matrix and stained respectively for β1 and β3 integrins. Linear invadosomes (white arrows) do not colocalize with integrins. β1 and β3: red; Tks5: green. Scale bar: 10 µm. Right panels, zoom (7×) of the white square. (C and D) MEFs were seeded on gelatin-FITC (C) or on mixed gelatin-FITC/collagen I matrix (D) and stained for Tks5 (green) and F-actin (red). Linear invadosomes and associated degradation are observed only in the presence of collagen I fibrils Gelatin-FITC: gray. Scale bar: 10 µm. (E) $\beta1^{-}/^{-}$ MEFs were seeded on the mixed matrix and exhibited functional linear invadosomes. Tks5: green; F-actin: red; gelatin-FITC: gray. Scale bar: 7 µm. (F) The same result was obtained with $\beta3^{-}/^{-}$MEFs. Tks5: green; F-actin: red; gelatin-FITC: gray. Scale bar: 5 µm. (G and H) Quantification of the number of linear invadosomes per micrometer squared and the fractional linear invadosomes area between WT, $\beta3^{-}/^{-}$, and $\beta1^{-}/^{-}$MEFs. NS: No significant difference.

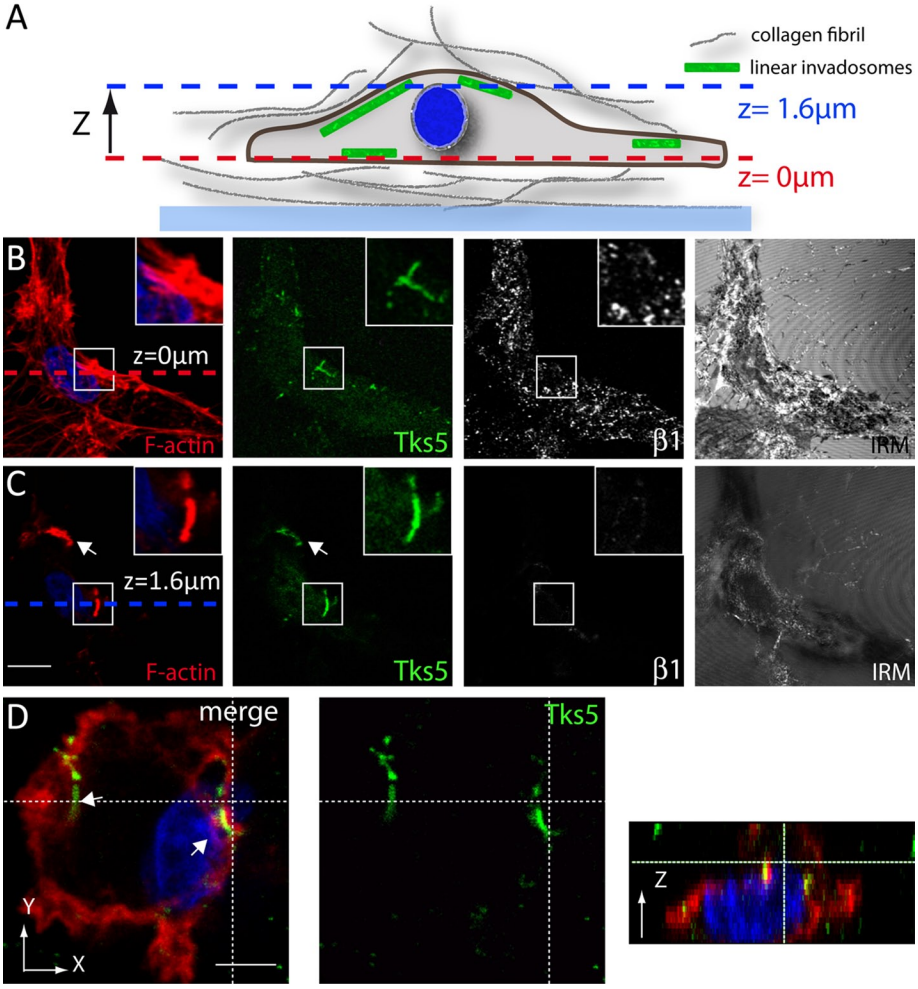

FIGURE 8: Linear invadosome formation in a three-dimensional environment. (A) Schematic representation of BAECs showing linear invadosomes (green lines) in a collagen I environment. The red and blue dotted lines correspond to focal planes of 0 and 1.6 µm, respectively. (B and C) Confocal and IRM images of BAECs reveal that linear invadosomes are localized at the bottom of the cell (Z: 0 µm) in contact with collagen I fibrils. F-actin: red; Tks5: green. Note that focal adhesions stained for β1 (gray levels) can be detected at the ventral part of BAECs, although they never colocalize with linear invadosomes. Linear invadosomes (white square) are present at the apical part of BAECs, as shown by the focal plane and selected IRM images (Z: 1.6 µm). Insets are zoomed images of the white squares. Scale bar: 5 µm. (D) Representative confocal images of BAECs embedded in a three-dimensional fibrillar collagen I matrix. F-actin (red) colocalizes with Tks5 (green) at linear invadosome level (white arrows), as depicted on merged image. Z-cut section reveals that linear invadosomes do exist in three dimensions. Nuclei: blue.

investigate the molecular mechanism allowing formation of linear invadosomes.

Like integrins themselves, integrin-associated proteins, such as vinculin or paxillin, are also not localized within linear invadosomes. Thus, linear invadosomes may be viewed as simplified but functional invadosomes containing only core elements, such as Tks5, which is necessary for linear invadosome formation. Recently it was shown that podosome cores can be formed in osteoclasts lacking the integrin adaptor kindlin-3$^{-/-}$ (Schmidt *et al.*, 2011). The presence of podosome cores in β1$^{-/-}$, β2$^{-/-}$, and αv$^{-/-}$ triple-null integrin knockout osteoclasts suggests that podosomes cores are integrin-independent structures (Schmidt *et al.*, 2011). Linear invadosomes retain their capacity to degrade ECM elements. The absence of adhesion proteins in linear invadosomes suggests that collagen I fibrils could bypass the role of podosome adhesion rings in terms of organization.

One of the major results of this study is the finding of a strong matrix degradation activity associated with linear invadosomes. In the case of Src-activated fibroblasts, this activity is even higher than the activity of invadosome rosettes observed on gelatin alone. These observations can be reconciled with the long-known finding that pro-MMP2 can be activated by the culture of cells on fibrillar collagen I, but not on any other type of ECM component (Azzam and Thompson, 1992; Ruangpanit *et al.*, 2001). Activation of the latent pro-MMP-2 zymogen is mainly due to membrane type MT1-MMP. Accordingly, we show here that linear invadosomes induced by collagen I fibrils can promote a concentration of MT1-MMP to linear invadosomes and an increase of gelatinolytic activity in a MT1-MMP–dependent process, and that the degradation activity is strictly limited to the vicinity of the collagen I fibrils. Our data also strongly suggest that linear invadosomes can degrade the underlying collagen I fibrils as well. Altogether, the results suggest that linear invadosomes can act as collagen I fibril sensors and are able to remodel the ECM.

Linear invadosomes were found in all cells tested. Their presence in normal cells (endothelial cells, fibroblasts, and macrophages) as well as in tumor cell lines suggests that they may have a major impact on physiological and pathological conditions. Since they are formed along the physiological form of collagen I and are found in a three-dimensional environment, this is compatible with a presence in vivo. We believe that they may represent one of the "physiological" configurations of invadosomes. The discovery of collagen I as a physiological inducer of invadosomes will probably help to better characterize their roles in vivo. Owing to their capacity to localize the degradation machinery along fibrils, linear invadosomes could be implicated in matrix remodeling and cell migration, either in physiological conditions, such as angiogenesis, or conditions in which collagen I is accumulated, such as fibrosis, atherosclerosis, and cancer.

MATERIALS AND METHODS

Reagents

Primary antibodies: anti-Tks5 (M-300) was from Santa Cruz Biotechnology (Santa Cruz, CA); anti-cortactin (clone 4F11), anti-phosphotyrosine (pY; clone 4G10), anti–MT1-MMP (clone LEM-2/15.8) were from Millipore (Billerica, MA). We also used anti–integrin β1 chain (clone 9EG7 and clone Ha2/5; BD PharMingen, San Diego, CA), β3 (cloneLuc.A5; Emfret, Eibelstadt, Germany), anti–N-WASP (clone 30D10; Cell Signaling Technology, Beverly, MA), anti-Arp2 (ab49674; Abcam, Cambridge, MA) and anti-vinculin (h-VIN-1; Sigma-Aldrich, St. Louis, MO). Paxillin antibody was a gift from E. Chevet (INSERM U1053, Bordeaux, France).

Secondary antibodies: Alexa Fluor 488, 546, 568 anti–rabbit, anti–mouse, and anti–rat antibodies were purchased from Invitrogen (Karlsruhe, Germany). FluoProbes 647H anti–rabbit and anti–mouse antibodies were obtained from Interchim (Montluçon, France). F-actin was stained with Phalloidin-FluoProbes 647 (Interchim) and Alexa Fluor 546 phalloidin (Invitrogen). Hoechst 34580 (Invitrogen) was used to stain nuclei. GM6001 was used as MMP inhibitor (Calbiochem, San Diego, CA). Imatinib and nilotinib were obtained from J. M. Pasquet (INSERM U1035, Bordeaux, France). To visualize the collagen I network, we labeled 0.4 mg/ml fibrillar collagen I with 10 µg/ml 5-(and 6)-carboxy-X-rhodamine succinimidyl ester (Invitrogen). The peptides RGDfV and RADfV were purchased from Enzo Life Sciences (Loerrach, Germany). M-CSF was kindly provided by P. Jurdic (ENS-Lyon-IGFL, France).

Cell culture

Src-3T3 cells, MEF $\beta3^{+/+}$ and $\beta3^{-/-}$, MEF $\beta1^{+/+}$ and $\beta1^{-/-}$, MEF MT1-MMP$^{+/+}$ and MT1-MMP$^{-/-}$, and CD44$^{-/-}$ were generous gifts from Sara A. Courtneidge (Burnham Institute for Medical Research, LaJolla, CA), Richard Hynes (The David H. Koch Institute for Integrative Cancer Research, Cambridge, MA), Martin Humphries (Wellcome Trust Centre for Cell-Matrix Research, Faculty of Life Sciences, Manchester, UK), Kenn Holmbeck (National Institute of Dental and Craniofacial Research, Bethesda, MD), and Richard Bucala (Department of Medicine, Yale University, New Haven, CT), respectively.

LSECs were isolated from male NMRI mice (6–8 wk; Charles River, Wilmington, MA) and from DDR2$^{-/-}$ mice provided by E. Olaso (Labrador *et al.*, 2001). Livers were mechanically disrupted and incubated with 2 mg/ml collagenase D (Roche, Mannheim, Germany) as previously described (Braet *et al.*, 2003). After isolation, LSECs were cultured in Clonetics EBM-2 medium supplemented with "Single Dots 4176" (Lonza, Breda, Germany). The M1 immortalized murine LSEC cell line (Matsuura *et al.*, 1998) was cultivated in the same medium as LSECs. HPAECs were cultivated in Clonetics EBM-2 medium supplemented with "Single Dots 4147" (Lonza). BAECs were cultured in endothelial cell growth medium MV supplemented with supplement mix (PromoCell, Heidelberg, Germany). Cells at passages 4–5 were used for experiments. HUVECs were cultivated in complete endothelial cell growth medium (PromoCell). PAECs were cultivated in Ham's F12 supplemented with 10% fetal calf serum (FCS; PAN-Biotech GmbH, Aidenbach, Germany) and 100 U/ml penicillin–streptomycin (Invitrogen).

MDA-MB-231, RAW 264.7, BHK-21, SVEC-4-10, Src-3T3, mouse embryonic fibroblasts (MEFs) $\beta3^{+/+}$, $\beta3^{-/-}$, MT1-MMP$^{+/+}$, and MT1-MMP$^{-/-}$, and primary HFF cells were maintained in DMEM GlutaMax-I 4.5 g/l (Invitrogen) supplemented with 10% FCS (PAN-Biotech GmbH) and 100 U/ml penicillin–streptomycin. Immortalized $\beta1^{-/-}$ MEFs were cultured as previously described (Parsons *et al.*, 2008). RAW were differentiated as previously described (Destaing *et al.*, 2003).

Transfection

Tks5-specific siRNA duplexes directed against the target sequence 5′-GAACGAAAGCGGCTGGTGG-3′ for siRNA1 or 5′-GCCAAAGCAAGGACGAGAT-3′ for siRNA2 and a control siRNA targeted against luciferase 5′-CGTACGCGGAATACTTCGA-3′ were purchased from Eurofins MWG Operons (Ebersberg, Germany). BAECs were seeded at 3×10^5 cells per 60-mm dish for 24 h and transfected with promofectin HUVEC (PromoKine, PromoCell). For DNA transfections, 2.5×10^5 PAECs were seeded on 60-mm dishes and were transfected the following day with 5 µg DNA using PromoFectin-Hepatocytes (Promokine, PromoCell) following the manufacturer's instructions. Tks5-GFP plasmid was kindly donated by S. Courtneidge. Lifeact Ruby construct was a generous gift from R. Wedlich-Soeldner (Martinsried, Germany; Riedl *et al.*, 2008).

Coatings and three-dimensional collagen I gels

Coverslips were coated with 0.4 mg/ml type I and III collagen (BD Biosciences, Bedford, MA), type IV collagen, vitronectin, fibronectin, laminin, or collagen I-FITC (Sigma) mixed in Dulbecco's phosphate-buffered saline (DPBS; Lonza) and incubated for 3 h at 37°C, after which they were washed gently in PBS before the addition of 2×10^4 cells. To obtain a monomeric form, collagen I was dissolved in 0.01 M acetic acid and allowed to polymerize for 3 h, and coverslips were washed three times in PBS.

For experiments on thick fibrillar collagen I coatings, BAECs were seeded on collagen I coatings (final concentration 0.4 mg/ml) without washing and allowed to penetrate the matrix for 16 h before fixation.

To produce three-dimensional collagen I matrices, rat tail collagen I solution was diluted in Hank's balanced salt solution, 0.25M $NaHCO_3$, 1M NaOH to a 2 mg/ml final collagen I concentration. 5×10^4 BAECs were embedded in collagen I solution and incubated 1 h at 37°C, and culture medium was added after gelation (Van Goethem *et al.*, 2010). The mixed matrix (gelatin + collagen I fibrils) was performed in two steps. First, glass coverslips were coated with FITC-gelatin, and after fixation with glutaraldehyde, recoating with collagen I fibrils.

Immunofluorescence, IRM, and live-cell imaging

Cells were fixed in 3.7% paraformaldehyde (pH 7.2) for 10 min, permeabilized with 0.2% Triton X-100 for 10 min, and incubated with various antibodies. F-actin distribution was revealed by Alexa Fluor 546 nm phalloidin. Cells were imaged with a confocal LSM 510 (Carl Zeiss Microimaging, Jena, Germany) or confocal SP5 (Leica, Leica Microsystems GmbH, Wetzlar, Germany) by using a 63×/numerical aperture (NA) 1.4 Plan-Neofluar objective. To prevent contamination between fluorochromes, each channel was imaged sequentially using the multitrack recording module before merging. Z-stack pictures were obtained using LSM 510 software. Three-dimensional reconstructions were obtained from Z-cut pictures, by using Imaris software (Bitplane, Zurich, Switzerland).

IRM of collagen I fibrils was imaged with a Plan-Neofluar Ph3, 63×/NA 1.25 oil immersion objective, mounted on a LSM 510 or Leica SP5.

For live-cell imaging, BAECs were seeded in 35-mm glass bottom dishes, then transferred to observation medium at 37°C as previously described (Destaing *et al.*, 2003). Dishes were placed on a thermostatted stage, and cells were imaged with a Zeiss laser-scanning microscope LSM510 (Axiovert 100M) and a 63×/NA 1.0 Zeiss Plan-Apochromat objective. LSM software was used to make AVI movies (see Supplemental Material; Chabadel *et al.*, 2007).

Zymography

Zymography and in situ zymography were performed as described in Hembry *et al.* (2007) and Seals *et al.* (2005), respectively.

Linear invadosome quantification

Confocal images of isolated cells were obtained using an SP5 confocal microscope (Leica) by using a 63×/NA 1.4 Plan Neo-Fluar objective. Cell surface area was measured upon phalloidin staining, and Tks5 staining was used as a marker for linear invadosomes. We developed a macro with ImageJ software that allowed measurement

of all required parameters of linear invadosomes: number, size (using the Feret diameter, the longest distance between any two points), and area (μm^2).

Statistics

Data were reported as mean ± SD. Statistical comparison between two groups was done using a paired *t* test. Differences were considered statistically significant if $p < 0.05$.

ACKNOWLEDGMENTS

We are grateful to S. Courtneidge for Tks5-GFP construct and Src-3T3; T. Matsuura for the M1 cell line; J. Saklatvala for the PAE cell line; R. Weldich-Soeldner for the Lifeact construct; R. Hynes, M. Humphries, R. Bucala, and K. Holmbeck for MEF knockout cells; and E. Olaso for the DDR2 knockout mice. We thank the Bordeaux Imaging Center for help in fluorescence quantification and P. Jurdic and E. Chevet for helpful discussions and critical comments on the manuscript. A.J. is supported by a predoctoral fellowship from the Ministère de l'Enseignement Supérieur et de la Recherche. C.B. is a recipient of grant ANR-06-BLAN-0362. This work was supported by grants from La Ligue Nationale contre le Cancer and Association pour la Recherche sur le Cancer/Institut National du Cancer. C.A.-R. and O.D. are supported by funding from "Equipe Labellisée 2010"; V.M. and J.R. are supported by funding from "Equipe Labellisée 2011."

REFERENCES

Abram CL, Seals DF, Pass I, Salinsky D, Maurer L, Roth TM, Courtneidge SA (2003). The adaptor protein fish associates with members of the ADAMs family and localizes to podosomes of Src-transformed cells. J Biol Chem 278, 16844–16851.

Albiges-Rizo C, Destaing O, Fourcade B, Planus E, Block MR (2009). Actin machinery and mechanosensitivity in invadopodia, podosomes and focal adhesions. J Cell Sci 122, 3037–3049.

Artym VV, Zhang Y, Seillier-Moiseiwitsch F, Yamada KM, Mueller SC (2006). Dynamic interactions of cortactin and membrane type 1 matrix metalloproteinase at invadopodia: defining the stages of invadopodia formation and function. Cancer Res 66, 3034–3043.

Azzam HS, Thompson EW (1992). Collagen-induced activation of the M(r) 72,000 type IV collagenase in normal and malignant human fibroblastoid cells. Cancer Res 52, 4540–4544.

Badowski C, Pawlak G, Grichine A, Chabadel A, Oddou C, Jurdic P, Pfaff M, Albiges-Rizo C, Block MR (2008). Paxillin phosphorylation controls invadopodia/podosomes spatiotemporal organization. Mol Biol Cell 19, 633–645.

Braet F, Muller M, Vekemans K, Wisse E, Le Couteur DG (2003). Antimycin A-induced defenestration in rat hepatic sinusoidal endothelial cells. Hepatology 38, 394–402.

Bravo-Cordero JJ, Oser M, Chen X, Eddy R, Hodgson L, Condeelis J (2011). A novel spatiotemporal RhoC activation pathway locally regulates cofilin activity at invadopodia. Curr Biol 21, 635–644.

Cardarelli PM, Cobb RR, Nowlin DM, Scholz W, Gorcsan F, Moscinski M, Yasuhara M, Chiang SL, Lobl TJ (1994). Cyclic RGD peptide inhibits α4 β1 interaction with connecting segment 1 and vascular cell adhesion molecule. J Biol Chem 269, 18668–18673.

Chabadel A, Banon-Rodriguez I, Cluet D, Rudkin BB, Wehrle-Haller B, Genot E, Jurdic P, Anton IM, Saltel F (2007). CD44 and β3 integrin organize two functionally distinct actin-based domains in osteoclasts. Mol Biol Cell 18, 4899–4910.

Cooper A (1970). Thermodynamic studies of the assembly in vitro of native collagen fibrils. Biochem J 118, 355–365.

David-Pfeuty T, Singer SJ (1980). Altered distributions of the cytoskeletal proteins vinculin and alpha-actinin in cultured fibroblasts transformed by Rous sarcoma virus. Proc Natl Acad Sci USA 77, 6687–6691.

Day E, Waters B, Spiegel K, Alnadaf T, Manley PW, Buchdunger E, Walker C, Jarai G (2008). Inhibition of collagen-induced discoidin domain receptor 1 and 2 activation by imatinib, nilotinib and dasatinib. Eur J Pharmacol 599, 44–53.

Destaing O, Block MR, Planus E, Albiges-Rizo C (2011). Invadosome regulation by adhesion signaling. Curr Opin Cell Biol 23, 597–606.

Destaing O, Planus E, Bouvard D, Oddou C, Badowski C, Bossy V, Raducanu A, Fourcade B, Albiges-Rizo C, Block MR (2010). β1A integrin is a master regulator of invadosome organization and function. Mol Biol Cell 21, 4108–4119.

Destaing O, Saltel F, Geminard JC, Jurdic P, Bard F (2003). Podosomes display actin turnover and dynamic self-organization in osteoclasts expressing actin-green fluorescent protein. Mol Biol Cell 14, 407–416.

Elbjeirami WM, Yonter EO, Starcher BC, West JL (2003). Enhancing mechanical properties of tissue-engineered constructs via lysyl oxidase crosslinking activity. J Biomed Mater Res A 66, 513–521.

Epstein EH, Jr., Munderloh NH (1975). Isolation and characterization of CNBr peptides of human $[\alpha1(III)]_3$ collagen and tissue distribution of $[\alpha1(I)]_2\alpha2$ and $[\alpha1(III)]_3$ collagens. J Biol Chem 250, 9304–9312.

Guegan F, Tatin F, Leste-Lasserre T, Drutel G, Genot E, Moreau V (2008). p190B RhoGAP regulates endothelial-cell-associated proteolysis through MT1-MMP and MMP2. J Cell Sci 121, 2054–2061.

Hai CM, Hahne P, Harrington EO, Gimona M (2002). Conventional protein kinase C mediates phorbol-dibutyrate-induced cytoskeletal remodeling in A7r5 smooth muscle cells. Exp Cell Res 280, 64–74.

Hembry RM, Atkinson SJ, Murphy G (2007). Assessment of gelatinase expression and activity in articular cartilage. Methods Mol Med 135, 227–238.

Jalkanen S, Jalkanen M (1992). Lymphocyte CD44 binds the COOH-terminal heparin-binding domain of fibronectin. J Cell Biol 116, 817–825.

Kelly T, Mueller SC, Yeh Y, Chen WT (1994). Invadopodia promote proteolysis of a wide variety of extracellular matrix proteins. J Cell Physiol 158, 299–308.

Labrador JP *et al.* (2001). The collagen receptor DDR2 regulates proliferation and its elimination leads to dwarfism. EMBO Rep 2, 446–452.

Leitinger B (2011). Transmembrane collagen receptors. Annu Rev Cell Dev Biol 27, 265–290.

Leitinger B, Hohenester E (2007). Mammalian collagen receptors. Matrix Biol 26, 146–155.

Li A, Dawson JC, Forero-Vargas M, Spence HJ, Yu X, Konig I, Anderson K, Machesky LM (2010). The actin-bundling protein fascin stabilizes actin in invadopodia and potentiates protrusive invasion. Curr Biol 20, 339–345.

Linder S (2007). The matrix corroded: podosomes and invadopodia in extracellular matrix degradation. Trends Cell Biol 17, 107–117.

Liu S, Yamashita H, Weidow B, Weaver AM, Quaranta V (2010). Laminin-332-β1 integrin interactions negatively regulate invadopodia. J Cell Physiol 223, 134–142.

Lizarraga F, Poincloux R, Romao M, Montagnac G, Le Dez G, Bonne I, Rigaill G, Raposo G, Chavrier P (2009). Diaphanous-related formins are required for invadopodia formation and invasion of breast tumor cells. Cancer Res 69, 2792–2800.

Matsuura T *et al.* (1998). High density culture of immortalized liver endothelial cells in the radial-flow bioreactor in the development of an artificial liver. Int J Artif Organs 21, 229–234.

Medalia O, Geiger B (2010). Frontiers of microscopy-based research into cell-matrix adhesions. Curr Opin Cell Biol 22, 659–668.

Monsky WL, Lin CY, Aoyama A, Kelly T, Akiyama SK, Mueller SC, Chen WT (1994). A potential marker protease of invasiveness, seprase, is localized on invadopodia of human malignant melanoma cells. Cancer Res 54, 5702–5710.

Moreau V, Tatin F, Varon C, Genot E (2003). Actin can reorganize into podosomes in aortic endothelial cells, a process controlled by Cdc42 and RhoA. Mol Cell Biol 23, 6809–6822.

Mueller SC, Ghersi G, Akiyama SK, Sang QX, Howard L, Pineiro-Sanchez M, Nakahara H, Yeh Y, Chen WT (1999). A novel protease-docking function of integrin at invadopodia. J Biol Chem 274, 24947–24952.

Nakahara H, Mueller SC, Nomizu M, Yamada Y, Yeh Y, Chen WT (1998). Activation of β1 integrin signaling stimulates tyrosine phosphorylation of p190RhoGAP and membrane-protrusive activities at invadopodia. J Biol Chem 273, 9–12.

Nascimento CF, de Siqueira AS, Pinheiro JJ, Freitas VM, Jaeger RG (2011). Laminin-111 derived peptides AG73 and C16 regulate invadopodia activity of a human adenoid cystic carcinoma cell line. Exp Cell Res 317, 2562–2572.

Ohuchi E, Imai K, Fujii Y, Sato H, Seiki M, Okada Y (1997). Membrane type 1 matrix metalloproteinase digests interstitial collagens and other extracellular matrix macromolecules. J Biol Chem 272, 2446–2451.

Osiak AE, Zenner G, Linder S (2005). Subconfluent endothelial cells form podosomes downstream of cytokine and RhoGTPase signaling. Exp Cell Res 307, 342–353.

Parsons M, Messent AJ, Humphries JD, Deakin NO, Humphries MJ (2008). Quantification of integrin receptor agonism by fluorescence lifetime imaging. J Cell Sci 121, 265–271.
Pfaff M, Jurdic P (2001). Podosomes in osteoclast-like cells: structural analysis and cooperative roles of paxillin, proline-rich tyrosine kinase 2 (Pyk2) and integrin αVβ3. J Cell Sci 114, 2775–2786.
Prockop DJ, Kivirikko KI (1984). Heritable diseases of collagen. N Engl J Med 311, 376–386.
Riedl J *et al.* (2008). Lifeact: a versatile marker to visualize F-actin. Nat Methods 5, 605–607.
Ruangpanit N, Chan D, Holmbeck K, Birkedal-Hansen H, Polarek J, Yang C, Bateman JF, Thompson EW (2001). Gelatinase A (MMP-2) activation by skin fibroblasts: dependence on MT1-MMP expression and fibrillar collagen form. Matrix Biol 20, 193–203.
Ruangpanit N, Price JT, Holmbeck K, Birkedal-Hansen H, Guenzler V, Huang X, Chan D, Bateman JF, Thompson EW (2002). MT1-MMP-dependent and -independent regulation of gelatinase A activation in long-term, ascorbate-treated fibroblast cultures: regulation by fibrillar collagen. Exp Cell Res 272, 109–118.
Sabri S *et al.* (2006). Deficiency in the Wiskott-Aldrich protein induces premature proplatelet formation and platelet production in the bone marrow compartment. Blood 108, 134–140.
Schmidt S, Nakchbandi I, Ruppert R, Kawelke N, Hess MW, Pfaller K, Jurdic P, Fassler R, Moser M (2011). Kindlin-3-mediated signaling from multiple integrin classes is required for osteoclast-mediated bone resorption. J Cell Biol 192, 883–897.
Seals DF, Azucena EF, Jr., Pass I, Tesfay L, Gordon R, Woodrow M, Resau JH, Courtneidge SA (2005). The adaptor protein Tks5/Fish is required for podosome formation and function, and for the protease-driven invasion of cancer cells. Cancer Cell 7, 155–165.
Shi X *et al.* (2006). CD44 is the signaling component of the macrophage migration inhibitory factor-CD74 receptor complex. Immunity 25, 595–606.
Shoulders MD, Raines RT (2009). Collagen structure and stability. Annu Rev Biochem 78, 929–958.
Tarone G, Cirillo D, Giancotti FG, Comoglio PM, Marchisio PC (1985). Rous sarcoma virus-transformed fibroblasts adhere primarily at discrete protrusions of the ventral membrane called podosomes. Exp Cell Res 159, 141–157.
Tatin F, Grise F, Reuzeau E, Genot E, Moreau V (2010). Sodium fluoride induces podosome formation in endothelial cells. Biol Cell 102, 489–498.
Tatin F, Varon C, Genot E, Moreau V (2006). A signalling cascade involving PKC, Src and Cdc42 regulates podosome assembly in cultured endothelial cells in response to phorbol ester. J Cell Sci 119, 769–781.
Theret N, Lehti K, Musso O, Clement B (1999). MMP2 activation by collagen I and concanavalin A in cultured human hepatic stellate cells. Hepatology 30, 462–468.
Van Goethem E, Poincloux R, Gauffre F, Maridonneau-Parini I, Le Cabec V (2010). Matrix architecture dictates three-dimensional migration modes of human macrophages: differential involvement of proteases and podosome-like structures. J Immunol 184, 1049–1061.
VanWinkle WB, Snuggs M, Buja LM (1995). Hypoxia-induced alterations in cytoskeleton coincide with collagenase expression in cultured neonatal rat cardiomyocytes. J Mol Cell Cardiol 27, 2531–2542.
Varon C, Tatin F, Moreau V, Van Obberghen-Schilling E, Fernandez-Sauze S, Reuzeau E, Kramer I, Genot E (2006). Transforming growth factor beta induces rosettes of podosomes in primary aortic endothelial cells. Mol Cell Biol 26, 3582–3594.
Wood GC, Keech MK (1960). The formation of fibrils from collagen solutions 1. The effect of experimental conditions: kinetic and electron-microscope studies. Biochem J 75, 588–598.
Xiao H, Eves R, Yeh C, Kan W, Xu F, Mak AS, Liu M (2009). Phorbol ester-induced podosomes in normal human bronchial epithelial cells. J Cell Physiol 218, 366–375.
Zambonin-Zallone A, Teti A, Carano A, Marchisio PC (1988). The distribution of podosomes in osteoclasts cultured on bone laminae: effect of retinol. J Bone Miner Res 3, 517–523.